Electrical Reverse Water Gas Shift by eREACT™
Technical whitepaper

ELECTRICAL REVERSE WATER GAS SHIFT BY eREACT™

TOPSOE

Prepared by:
Sebastian Thor Wismann, Kasper Emil Larsen,
Peter Mølgaard Mortensen from Topsoe A/S

"This is the pre-peer reviewed version of the following article: Electrical Reverse Shift: Sustainable CO_2 Valorization for Industrial Scale, which has been published in final form at https://doi.org/10.1002/anie.202109696. This article may be used for non-commercial purposes in accordance with Wiley Terms and Conditions for Use of Self-Archived Versions."

CONTENTS

EXECUTIVE SUMMARY

Utilization of CO_2 is a requirement for a sustainable production of carbon-based chemicals. Reverse water gas shift (RWGS) can valorize CO_2 by reaction with hydrogen to produce a synthesis gas compatible with existing industrial infrastructure. Fully electrified reverse water gas shift by eREACT™ was achieved using catalyzed hardware with integrated ohmic heating and a non-selective catalyst at industrially relevant conditions. In a representative experiment at 900°C, the composition is equivalent to a RWGS selective catalyst, producing a synthesis gas with a H_2/CO ratio of 2.0, ideal for production of sustainable fuel by the Fischer-Tropsch synthesis. Using a non-selective catalyst was found superior over a selective RWGS catalyst due to higher activity and suppression of carbon formation. The eREACT™ catalyst is found to provide a preferential route for production of synthesis gas for any relevant H_2/CO ratio, enabling production of sustainable carbon-based chemicals with high carbon efficiency from CO_2 and renewable electricity.

INTRODUCTION

Growing environmental concerns have clarified that a reduction in CO_2 emissions may not be enough to reach the Paris agreement, and sustainable products must therefore utilize CO_2 as well [1]. While some products based on fossil fuels can be fully electrified, liquid fuels with high energy density are still required in most scenarios [1]. Converting just 2.5% of emitted CO_2 to hydrocarbon-based fuels with renewable energy could cover the entire aviation sector today [2]. Another growing necessity is economic large-scale storage of renewable energy to bridge the gap between intermittent supply and demand inherent to renewable energy production, be it wind or solar [3].

Today, only few processes at industrial scale can valorize CO_2. Dry reforming, converting mixtures of CO_2 and methane can in theory yield a desirable synthesis gas; however, to avoid formation of carbon, industrial applications today are operated with addition of steam [4]. A two-stage chemical looping process can produce targeted H_2/CO ratios by reducing CO_2 using metal oxide intermediates [5]. Reforming in plasma can operate with production of solid carbon and have been realized at a commercial scale, however with limited energy efficiency [6]. CO_2 can also be reduced electrochemically, though improved activity and stability are required for industrial applications [7]. Co-electrolysis of H_2O and CO_2 in SOEC can operate with high efficiency [8], though CO concentration is limited by the risk of localized carbon formation from the Boudouard reaction [9, 10].

Reverse water gas shift (RWGS, Reaction 1) can convert CO_2 and (green) hydrogen from e.g. electrolysis to a synthesis gas with desired composition to enable high carbon efficiency with the existing industrial framework.

$$CO_2 + H_2 \rightleftharpoons CO + H_2O \quad \Delta H_r^\circ = 41\ \text{kJ/mol} \qquad (1)$$

A RWGS selective catalyst can be used to suppress the strongly exothermic methanation reaction inhibiting formation of methane (Reaction 2).

$$CO + 3H_2 \rightleftharpoons CH_4 + H_2O \quad \Delta H_r^\circ = -206\ \text{kJ/mol} \qquad (2)$$

However, methane slip generally increases with temperature for most WGS catalysts, and product separation is required to reach a high CO_2 conversion [11]. An exemption to this was demonstrated by *Wang et al.* on a nickel-based catalyst with no methane slip at 1:1 H_2:CO_2 at 600 to 750°C [12]. RWGS selective catalysts are typically based on highly dispersed metal supported on promoted supports or oxides [11, 13]. *He et al.* recently demonstrated an ideal selectivity on nanostructured MnO_2 catalyst at 1:1 H_2:CO_2 thermally stable up to 850°C [14].

Non-selective catalysts, such as Ni, Ru, or Rh, generally have a lower activation energy for the RWGS reaction that combined with higher metal loadings and high temperature operation yields conversion rates orders of a magnitude higher than WGS selective catalyst [11, 14–18]. Byproduct formation of methane can be converted to CO at high temperatures through the steam methane reforming reaction (reverse methanation, Reaction 2) to obtain a desirable H_2/CO ratio for subsequent processes [19]. Typical end products from syngas are synthetic fuels from the Fischer-Tropsch process, acetic acid, oxo-alcohols, or methanol [13].

Electrically heated catalysis was evaluated pronounced preferential specifically for facilitating the endothermic RWGS reaction scheme, as using e.g., a fired approach counteracts the purpose of CO_2 utilization by having an associated CO_2 emission.

In this work, an electrical RWGS approach was used utilizing catalyzed hardware, comprised of a metallic structure with a catalytically active porous washcoat. An electrical potential difference draws a current through the metallic support, heating the catalytic washcoat by ohmic losses as described in the previous work from our group [20, 21]. The short characteristic length scale alleviates heat transfer limitations opposed to conventional reactors with catalyst pellets heated outside-in [21]. The integrated heating, low thermal mass, and small thermal gradients enable flexible operation with fast start-up, in contrast to externally fired reactors [22].

EXPERIMENTAL

In a pressurized bench-scale reactor, a FeCrAl-alloy structure washcoated with a porous zirconia-based coat and impregnated with a nickel catalyst is heated similar to the previous work [20, 21]. This nickel-based catalyst configuration opens for the methanation reaction (Reaction 2). For the experimental data presented here, the reactor was operated at industrially relevant conditions, with a feed consisting of 30% CO_2 and 70% H_2 (2.25 $H2_2$:CO_2) at 10 barg, preheated to 200°C, aiming for a H_2/CO ratio of 2, as desired for the Fischer-Tropsch process [19].

RESULTS AND DISCUSSION

Figure 1 summarizes experimental data from operation of the eREACT™ reactor together with equilibrium calculations at non-selective conditions. The methane fraction in the product reaches a maximum around 645°C, which decreases again at higher temperatures. The data illustrate that the methane fraction is below the thermodynamic equilibrium content up to 800°C while the CO fraction is above, which indicates the reactions are sequential, and that moderate temperatures are required to initiate the RWGS reaction (Reaction 1). It is expected that the RWGS reaction is faster than the methanation reaction, and the data underline that dissociation of CO is necessary for the methanation reaction, as also described by *Wind et al*. [23]. Above 900°C, methane slip decreases to less than 0.2%, yielding a product gas very close to an ideal RWGS selective catalyst [12, 14].

The CO_2 conversion, calculated from the carbon balance, increases with temperature to a thermodynamic plateau above 1000°C. With an industrially negligible methane slip above 900°C (<0.2%), the H_2/CO ratio is determined by the feed composition as the reactions run towards equilibrium, here a 2.25 H_2:CO_2 feed ratio yields a H_2/CO ratio of 2, ideal for the FT-process (Figure 2).

FIGURE 1: Product gas composition as a function of temperature

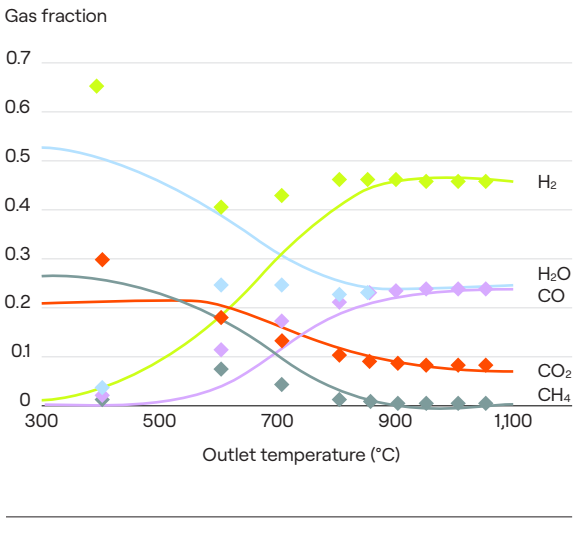

The full lines are the thermodynamic equilibrium for a non-selective catalyst. Measurements between 400 and 600°C cannot be obtained due to the exothermicity of the methanation reaction. 10 barg, 2.25 H_2:CO_2 feed, 200°C inlet temperature.

FIGURE 2: CO_2 conversion, H_2/CO ratio, and methane slip as a function of temperature

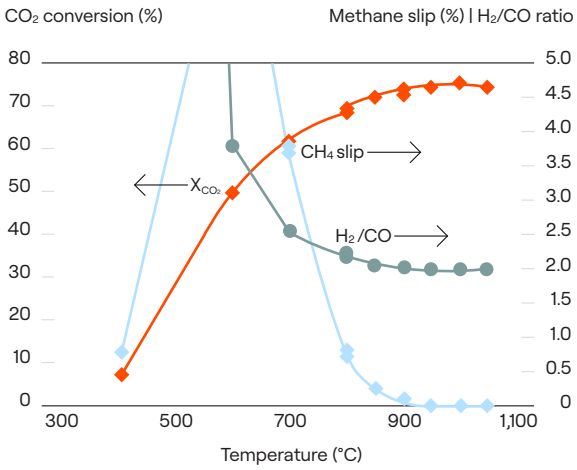

10 barg, 2.25 H_2:CO_2 feed, 200°C inlet temperature.

When using a nickel-based catalyst, carbon formation can take place, making it crucial to keep carbon potential low [19]. For eREACT™ at RWGS conditions, the most critical of the carbon forming reactions is the exothermic CO reduction (Reaction 3), where the absence of water in the feed will yield high carbon forming potentials when the RWGS reaction is initiated. The other typical carbon forming reactions are methane decomposition (Reaction 4) and the Boudouard reaction (Reaction 5).

$$CO + H_2 = C + H_2O \quad \Delta H_r^\circ = -130\ \text{kJ/mol} \quad (3)$$
$$CH_4 = C + 2H_2 \quad \Delta H_r^\circ = 75\ \text{kJ/mol} \quad (4)$$
$$2CO = C + CO_2 \quad \Delta H_r^\circ = -171\ \text{kJ/mol} \quad (5)$$

The risk of carbon formation can be assessed from the thermodynamics. If the carbon activity is below unity, there is no thermodynamic potential to form carbon. If the catalyst is sufficiently active, the carbon potential should be evaluated for the equilibrated gas, based on the assumption that thermodynamic equilibrium is achieved on the surface of the nanoparticle and a general strive of the system to achieve the overall lowest energy state [19]. The equilibrated carbon potential is independent of carbon forming reaction. For the CO reduction, the equilibrated carbon potential is defined as:

$$a^{eq}_{c,co\ red} = K_{eq} \cdot \frac{y_{CO} \cdot y_{H_2}}{y_{H_2O}} \cdot P \Big|_{eq}$$

Where K_{eq} is the equilibrium constant [19] and P the absolute pressure. Figure 3 shows the calculated carbon activity for the cases with and without a selective RWGS catalyst. For an ideal RWGS selective catalyst, the equilibrated carbon potential exceeds unity by several orders of magnitude below 800°C, indicating that any carbon-forming site would yield carbon. It should be mentioned here that high-temperature RWGS selective catalysts typically are based on oxides or finely dispersed particles and formation of carbon will have a high activation energy, which may kinetically inhibit the formation [24, 25].

Compared with the RWGS selective case, the carbon activity on a non-selective catalyst is suppressed by two phenomena. First, the methanation reaction will convert CO to methane and steam. This quickly reduces the CO/H_2O ratio, suppressing the carbon potential from CO reduction (Reaction 3). Secondly, the methanation is exothermic, quickly elevating the temperature outside a region where the carbon activity exceeds unity. Consequently, the equilibrated carbon potential for the non-selective catalyst is below unity for the entire operating regime when using catalyst specific equilibrium data (Whisker type carbon), which is the threshold for practical observation of carbon formation in steam reforming environment [19].

FIGURE 3: Equilibrated carbon activity

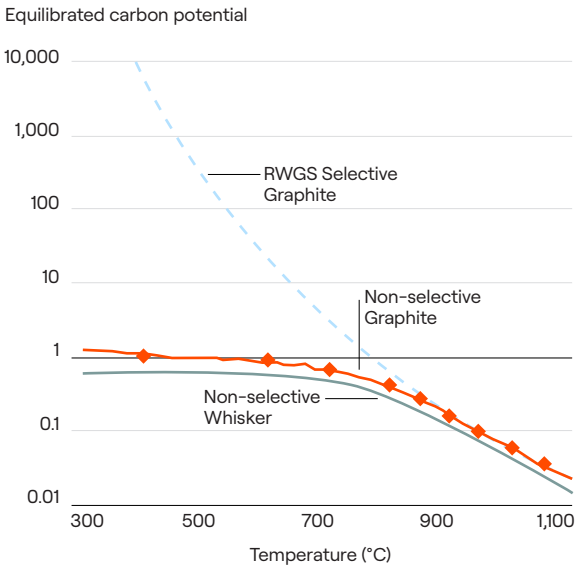

Equilibrated carbon activity calculated for an ideal RWGS selective catalyst and a non-selective catalyst. For the non-selective, the potential for whisker carbon on nickel is included.

To elucidate the phenomena of the eREACT™ reactor, a CFD model was set up. The model assumes the reactor is adiabatic, which is deemed a reasonable approximation for industrial scale reactor with integrated heating. Details of the CFD model can be found in the previous publications [20, 21].

The non-selective catalyst yields an initially steep temperature profile due to the exothermic methanation that levels off as the equilibrium temperature is reached (ca. 620°C at 10 barg), after which the reforming reaction takes over, converting the methane back to CO (Figure 4). For comparison, the temperature profile for an ideal RWGS selective catalyst was simulated (complete suppression of the methanation reaction while using the activation energy of a nickel catalyst for RWGS [16]), which yields a much steadier temperature profile due to the significantly different reaction enthalpy. According to the first law of thermodynamics, the "free energy" supplied by the methanation is balanced by the heat required to revert the reaction, yielding comparable conversion and outlet temperatures with an equivalent supply of heat for the two cases. The simulation with a non-selective catalyst has an exit temperature ca. 40°C higher due to a 0.2% methane slip. The higher temperature results in a slightly higher CO selectivity.

FIGURE 4: Predicted averaged temperature profile for an adiabatic reactor

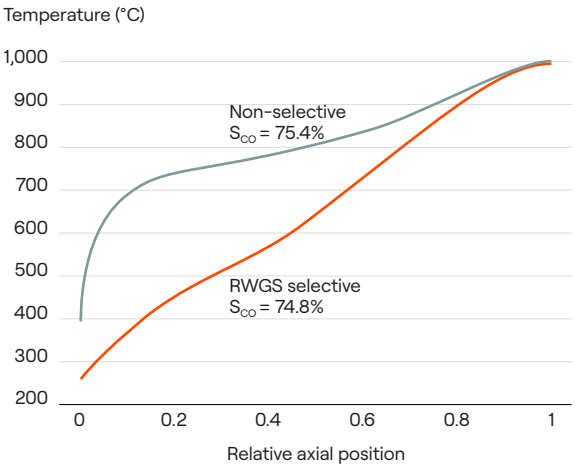

Predicted averaged temperature profile for an adiabatic reactor for a RWGS selective and a reforming active catalyst. Slightly higher CO activity is achieved with the reforming active catalyst due to the higher temperature. Model conditions: 36 Nl/h, 16.1 W, 200°C inlet, 10 barg.

Another benefit of the steep initial temperature profile is the exponential temperature dependence for the reaction rate. For the RWGS selective catalyst, the initial part of the reactor is cooled by the endothermic RWGS reaction (Reaction 1), in contrast to the rapid heating from the exothermic heating from methanation enabled with a non-selective catalyst. This yields a low reaction rate for the RWGS selective catalyst, resulting in a lower CO fraction at equivalent axial position compared to a non-selective catalyst, as illustrated in Figure 5. With the adiabatic assumption of the CFD model, the heat supplied from methanation using a non-selective catalyst is sufficient to initiate the reforming reaction (reverse of Reaction 2) at the top of the reactor. For the RWGS selective catalyst, the majority of the reaction is carried out near the center of the reactor, where with the non-reactive catalyst, the bulk of the reaction occurs at the inlet.

FIGURE 5: Modelled CO fraction

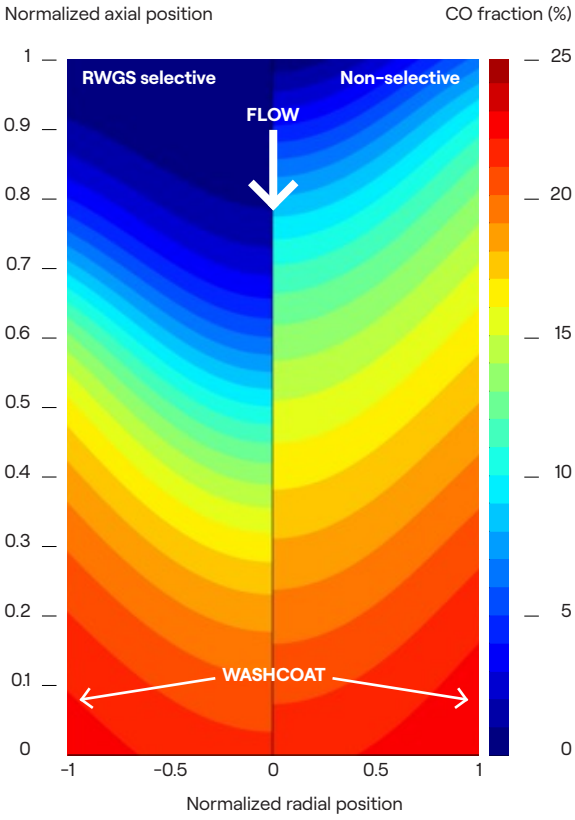

Modelled CO fraction in a channel with a RWGS selective or non-selective catalyst. The illustration is not to scale. Conditions equivalent to Figure 4.

CONCLUSION

Abatement of CO_2 emissions may be insufficient to mitigate severe environmental impact. Reverse shift of CO_2 and hydrogen enables production of a sustainable syngas compatible with existing industrial infrastructure for carbon-based chemicals. The eREACT™ system enables valorization of CO_2 with no associated emissions. Using a reforming active catalyst benefits the temperature profile, suppresses carbon formation, provides higher intrinsic activity, and mitigates methane slip when utilizing the features of ohmic heating to reach temperatures of the exit gas above 900°C. eREACT™ provides a route for production of sustainable chemicals based on renewable electricity, converting CO_2 and hydrogen to a syngas compatible with the existing industrial infrastructure.

REFERENCES

(1) United Nations Environment Programme, Emissions Gap Emissions Gap Report 2020, 2020. https://www.unenvironment.org/interactive/emissions-gap-report/2019/.

(2) B. Graver, K. Zhang, D. Rutherford, CO_2 emissions from commercial aviation, 2018, Int. Counc. Clean Transp. 2019. (2019) 13.

(3) H. Lund, P.A. Østergaard, D. Connolly, I. Ridjan, B.V. Mathiesen, F. Hvelplund, J.Z. Thellufsen, P. Sorknses, Energy storage and smart energy systems, Int. J. Sustain. Energy Plan. Manag. 11 (2016) 3–14. https://doi.org/10.5278/ijsepm.2016.11.2.

(4) P.M. Mortensen, I. Dybkjær, Industrial scale experience on steam reforming of CO<inf>2</inf>-rich gas, Appl. Catal. A Gen. 495 (2015) 141–151. https://doi.org/10.1016/j.apcata.2015.02.022.

(5) A.E. Ramos, D. Maiti, Y.A. Daza, J.N. Kuhn, V.R. Bhethanabotla, Co, Fe, and Mn in La-perovskite oxides for low temperature thermochemical CO_2 conversion, Catal. Today. 338 (2019) 52–59. https://doi.org/10.1016/j.cattod.2019.04.028.

(6) A. V Surov, S.D. Popov, V.E. Popov, D.I. Subbotin, E.O. Serba, V.A. Spodobin, G. V Nakonechny, A. V Pavlov, Multi-gas AC plasma torches for gasification of organic substances, Fuel. 203 (2017) 1007–1014. https://doi.org/10.1016/j.fuel.2017.02.104.

(7) Q. Lu, F. Jiao, Electrochemical CO_2 reduction: Electrocatalyst, reaction mechanism, and process engineering, Nano Energy. 29 (2016) 439–456. https://doi.org/10.1016/j.nanoen.2016.04.009.

(8) A. Hauch, R. Küngas, P. Blennow, A.B. Hansen, J.B. Hansen, B. V. Mathiesen, M.B. Mogensen, Recent advances in solid oxide cell technology for electrolysis, Science (80-.). 370 (2020). https://doi.org/10.1126/science.aba6118.

(9) J.D. Duhn, A.D. Jensen, S. Wedel, C. Wix, Optimization of a new flow design for solid oxide cells using computational fluid dynamics modelling, J. Power Sources. 336 (2016) 261–271. https://doi.org/10.1016/j.jpowsour.2016.10.060.

(10) Y. Tao, S.D. Ebbesen, M.B. Mogensen, Carbon Deposition in Solid Oxide Cells during Co-Electrolysis of H_2O and CO_2 , J. Electrochem. Soc. 161 (2014) F337–F343. https://doi.org/10.1149/2.079403jes.

(11) Y.A. Daza, J.N. Kuhn, CO_2 conversion by reverse water gas shift catalysis: Comparison of catalysts, mechanisms and their consequences for CO_2 conversion to liquid fuels, RSC Adv. 6 (2016) 49675–49691. https://doi.org/10.1039/c6ra05414e.

(12) L. Wang, H. Liu, Y. Liu, Y. Chen, S. Yang, Effect of precipitants on Ni-CeO_2 catalysts prepared by a co-precipitation method for the reverse water-gas shift reaction, J. Rare Earths. 31 (2013) 969–974. https://doi.org/10.1016/S1002-0721(13)60014-9.

(13) D.B. Pal, R. Chand, S.N. Upadhyay, P.K. Mishra, Performance of water gas shift reaction catalysts: A review, Renew. Sustain. Energy Rev. 93 (2018) 549–565. https://doi.org/10.1016/j.rser.2018.05.003.

(14) Y. He, K.R. Yang, Z. Yu, Z.S. Fishman, L.A. Achola, Z.M. Tobin, J.A. Heinlein, S. Hu, S.L. Suib, V.S. Batista, L.D. Pfefferle, Catalytic manganese oxide nanostructures for the reverse water gas shift reaction, Nanoscale. 11 (2019) 16677–16688. https://doi.org/10.1039/c9nr06078b.

(15) X. Yang, X. Su, X. Chen, H. Duan, B. Liang, Q. Liu, X. Liu, Y. Ren, Y. Huang, T. Zhang, Promotion effects of potassium on the activity and selectivity of Pt/zeolite catalysts for reverse water gas shift reaction, Appl. Catal. B Environ. 216 (2017) 95–105. https://doi.org/10.1016/j.apcatb.2017.05.067.

(16) J.G. Xu, G.F. Froment, Methane steam reforming, methanation and water-gas shift .1. Intrinsic Kinetics, Aiche J. 35 (1989) 88–96. https://doi.org/10.1002/aic.690350109.

(17) X. Chen, X. Su, H. Duan, B. Liang, Y. Huang, T. Zhang, Catalytic performance of the Pt/TiO2 catalysts in reverse water gas shift reaction: Controlled product selectivity and a mechanism study, Catal. Today. 281 (2017) 312–318. https://doi.org/10.1016/j.cattod.2016.03.020.

(18) J. Wei, E. Iglesia, Mechanism and Site Requirements for Activation and Chemical Conversion of Methane on Supported Pt Clusters and Turnover Rate Comparisons among Noble Metals, J. Phys. Chem. B. 108 (2004) 4094–4103. https://doi.org/10.1021/jp036985z.

(19) J. Rostrup-Nielsen, L.J. Christiansen, Concepts in Syngas Manufacture, Imperial College Press, 2011.

(20) S.T. Wismann, J.S. Engbæk, S.B. Vendelbo, F.B. Bendixen, W.L. Eriksen, K. Aasberg-petersen, C. Frandsen, I. Chorkendorff, P.M. Mortensen, Electrified methane reforming: A compact approach to greener industrial hydrogen production, Science (80-.). 364 (2019) 756–759. https://doi.org/10.1126/science.aaw8775.

(21) S.T. Wismann, J.S. Engbæk, S.B. Vendelbo, W.L. Eriksen, C. Frandsen, P.M. Mortensen, I. Chorkendorff, Electrified methane reforming: Understanding the dynamic interplay, Submitted. (2019).

(22) Sebastian T. Wismann, J.S. Engbæk, S.B. Vendelbo, W.L. Eriksen, C. Frandsen, P. Mortensen, I. Chorkendorff, Electrified reforming - Elucidating transient phenomena, (2021).

(23) T.L. Wind, H. Falsig, J. Sehested, P.G. Moses, T.T.M. Nguyen, Comparison of mechanistic understanding and experiments for CO methanation over nickel, J. Catal. 342 (2016) 105–116. https://doi.org/10.1016/j.jcat.2016.07.014.

(24) L. Wang, H. Liu, Y. Chen, S. Yang, Reverse water–gas shift reaction over co-precipitated Co–CeO_2 catalysts: Effect of Co content on selectivity and carbon formation, Int. J. Hydrogen Energy. 42 (2017) 3682–3689. https://doi.org/10.1016/j.ijhydene.2016.07.048.

(25) H.S. Bengaard, J.K. Nørskov, J. Sehested, B.S. Clausen, L.P. Nielsen, A.M. Molenbroek, J.R. Rostrup-Nielsen, Steam reforming and graphite formation on Ni catalysts, J. Catal. 209 (2002) 365–384. https://doi.org/10.1006/jcat.2002.3579.

Founded in 1940, Topsoe is a global leader in developing solutions for a decarbonized world, supplying technology, catalysts, and services for worldwide energy transition.

Our mission is to combat climate change by helping our partners and customers achieve their decarbonization and emission-reduction targets, including those in challenging sectors: aviation, shipping, and production of crucial raw materials.

From low-carbon or zero-carbon chemicals to renewable fuels and plastic upcycling, we are uniquely positioned to aid humanity in realizing a sustainable future.

Topsoe is headquartered in Denmark, with 2,100 employees serving customers all around the globe. To learn more, visit topsoe.com

Get in touch today
topsoe.com/contact

TOPSOE

Topsoe A/S
Haldor Topsøes Allé 1
2800 Kongens Lyngby
Denmark

Tel. +45 45 27 20 00
CVR no. 41 85 38 16

Topsoe A/S,
CVR 41853816
0352.2022/Rev.1